

The effect of linear and logarithmic discretization on the current through noninteracting quantum dots



Bachelorarbeit
an der Fakultät für Physik
der Ludwig-Maximilians-Universität
München

vorgelegt von
Konstantin Kröniger
aus Unterammergau

München, den 06. August 2012

Gutachter: Prof. Dr. Jan von Delft

Abstract

The objective of this Bachelor thesis is to examine the effect linear and logarithmic discretizations of continuous energy bands have on the current through a noninteracting quantum dot. This will be done by comparing with the exact current results obtained by an analytical treatment of the considered system.

Contents

Introduction	3
I Many particle systems	5
1 Hilbert space and Hilbert space basis	5
2 Second Quantization	6
3 Statistical Mechanics	7
4 Greenfunctions	8
II Current through a quantum dot coupled to leads: Theoretical approach	12
5 Assumptions	12
6 Base and Hamiltonian	12
7 Current I	13
III Current through a quantum dot coupled to leads: Simulation	22
8 Determining $I(t)$	22
9 Linear discretization	26
10 Results (linear discretization)	31
11 Logarithmic discretization	33
12 Results (logarithmic discretization)	34
13 $V/\Gamma > 1$ and $\Lambda = 2$	36

Conclusion	39
Appendix	40
A Programs	40
Acknowledgements	46

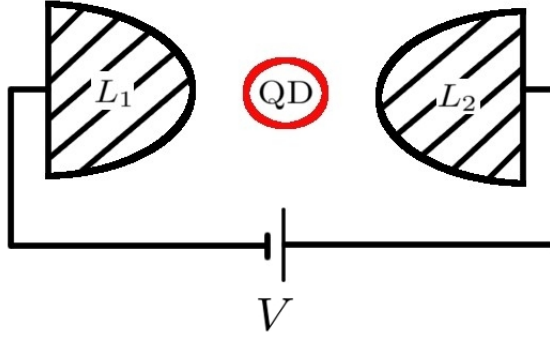


Figure 1: Considered system of a quantum dot (QD) between two leads (L_1 , L_2) with the electrical potential V applied to them.

Introduction

In the following work our main aim is to discover how the kinematic properties of a many body system are dependent on different discretizations of a continuous energyband. For this purpose, our model system will be a quantum dot¹(QD), coupled to two leads (L_1 , L_2). The kinematic quantity, we want to probe is the tunneling current through the quantum dot, when we apply an electrical potential (V) to the leads (see figure 1).

We consider our system temperature T to be 0(Kelvin). Therefore we can depict our problem in the energyspace as in figure 2. Our electrons occupy states up to the fermi edge, which is equal to the chemical potential μ . Here, the left lead's energy levels are filled till μ_l , and the right lead's levels are filled till μ_r ². The single energy level of the quantumdot is denoted by ϵ_d . For simplicity we will assume that there are no interactions between electrons, e.g. no Coloumb interaction. Now our approach will be the following:

Part I of the work shortly introduces the techniques, which are needed for the treatment of our model system (compare with Ref.[3]).

In part II, we will derive an analytic formular for the current-electrical potential dependence, which is possible as we only have one energy level in the quantumdot and as our electrons are noninteracting (compare with Ref.[2]). The theoretical result will than be used to probe the quality of the different discretizations used in a numerical simulation.

Part III treats the simulation of our system with two different discretizations and compares the results one attains in the different cases. The energy bands will be discretized the following two ways:

- The first discretization is equally choosen on both leads with linear discretization in the interval $[\mu_r, \mu_l]$ of interest. Large energies outside this interval will be discretized more crudely, following a logarithmic discretization scheme. We denote this discretization as "linear" discretization.
- The second discretization is choosen logarithmically relative to the chemical potential of each

¹i.e. a quantumsystem, which consists of a small amount of states, electrons can occupy, when "sitting" in the quantumdot.

²The electrical potential V of figure 1 hence gets: $eV = \mu_l - \mu_r$

lead motivated by the numerical renormalization group (NRG) (see Ref.[1]). As $\mu_l \neq \mu_r$, the discretizations are different on both leads. This discretization will be denoted "logarithmic" discretization.

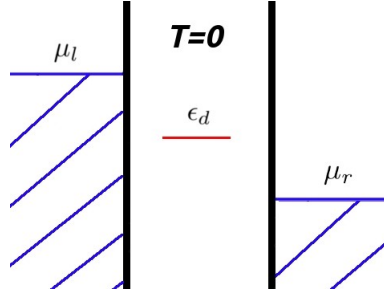


Figure 2: System of interest for temperature $T=0$ in energyspace.

Part I

Many particle systems

As our system of interest is a fermionic many particle system, we give a short review of the Hilbert space and the Hilbert space basis we are going to work with, the second quantization formalism, equilibrium Greenfunctions and the Keldysh-formalism, as we want to treat a nonequilibrium system.

1 Hilbert space and Hilbert space basis

The Hilbert space we are going to describe our N -particle system with is the Hilbert space

$$\mathcal{H} \subset \mathcal{H}^{(1)} \otimes \dots \otimes \mathcal{H}^{(N)} \quad (1)$$

where $\mathcal{H}^{(i)}$ is the one particle Hilbert space of the i -th particle. Given fermions, this Hilbert space describes antisymmetric statekets.

For our orthonormal basis (ONB), we will use the eigenvectors of a hermitian operator with discrete eigenvalues $\alpha_1, \alpha_2, \dots$, e.g. the Hamilton operator.

Then the ONB \mathcal{B} has the following form:

$$\mathcal{B} = \{|N; n_1 n_2 \dots\rangle\} \quad (2)$$

where N is the total particle number of our system and n_i is the number of particles in the eigenstate according to the eigenvalue α_i . As we work with noninteracting fermions, we can neglect their spin, and therefore only allow:

$$n_i \in \{0, 1\} \quad (3)$$

according to the Pauli principle.

2 Second Quantization

As usual the creation (c_r^\dagger) and annihilation (c_r) operators are defined as:

$$\begin{aligned} c_r^\dagger &: \mathcal{H}^{(-),N-1} \longrightarrow \mathcal{H}^{(-),N} \\ |N; n_1 n_2 \cdots n_r \cdots \rangle &\longmapsto (-1)^{N_r} \delta_{n_r 0} |N+1; n_1 n_2 \cdots n_r + 1 \cdots \rangle \end{aligned} \quad (4)$$

where $N_r = \sum_{i=1}^{r-1} n_i$

and $c_r \equiv (c_r^\dagger)^\dagger$, therefore:

$$c_r |N; n_1 n_2 \cdots n_r \cdots \rangle = (-1)^{N_r} \delta_{n_r 1} |N-1; n_1 n_2 \cdots n_r - 1 \cdots \rangle \quad (5)$$

The creation operator c_r^\dagger creates a particle in the eigenstate corresponding to the eigenvalue α_r and the annihilation operator annihilates one.

The occupation operator of the r 'th eigenstate \hat{n}_r is defined as:

$$c_r^\dagger c_r = \hat{n}_r \quad (6)$$

By definition, one gets the fundamental anticommutation relations:

$$\{c_k^\dagger, c_l^\dagger\} = \{c_k, c_l\} = 0 \quad \forall k, l \quad (7)$$

$$\{c_k, c_l^\dagger\} = \delta_{kl} \quad \forall k, l \quad (8)$$

where $\{\cdot, \cdot\}$ symbolizes the anticommutator, defined by:

$$\{A, B\} = AB + BA \quad (9)$$

With this relations one can derive the following commutator relations, for the creation and annihilation operators:

$$[c_k, c_l^\dagger c_m] = \delta_{kl} c_m \quad (10)$$

$$[c_k^\dagger c_k, c_l^\dagger c_m] = \delta_{kl} c_k^\dagger c_m - \delta_{km} c_l^\dagger c_k \quad (11)$$

where the commutator $[\cdot, \cdot]$ is defined by:

$$[A, B] = AB - BA \quad (12)$$

Next we want to transform operators in the second quantization formalism. As our system is noninteracting we will only need single particle operators, which have the form:

$$A = \sum_{n=1}^N \mathbf{1}^{n-1} \otimes A^{(n)} \otimes \mathbf{1}^{N-n} \equiv \sum_{n=1}^N A^{(n)} \quad (13)$$

with the $A^{(n)}$ only operating on the Hilbert space \mathcal{H}_n of a single particle.

Now using a ONB $\mathcal{D} = \{|i\rangle\}$ of the Hilbert space of one of our particles, we can write the single particle operator as:

$$A = \sum_{i,k \in \{|i\rangle\}} \langle i|A_{op}|k\rangle c_i^\dagger c_k \quad (14)$$

where A_{op} is the one-particle operator operating in the Hilbert space of a single particle.

3 Statistical Mechanics

Because we will do equilibrium theory as well, we will have to use statistical mechanics. We briefly review the facts, which are important for this work.

For a grand canonical ensemble the expectation value of an operator A at $t = \infty$ can be written as:

$$\langle A \rangle \equiv {}_{eq} \langle \psi | A | \psi \rangle_{eq} = \frac{1}{Z} \text{Tr} \{ \rho A \} \quad (15)$$

where

- $\rho = e^{-\beta(\hat{H} - \mu\hat{N})}$ is the density operator
- $Z = \text{Tr} \{ \rho \}$ is the partition function
- $\beta = \frac{1}{k_B T}$, where T is the temperature and k_B is the Boltzmann constant
- \hat{H} is the Hamilton operator, describing our system
- μ is the chemical potential of our system
- \hat{N} is the particle number operator

One important result one can obtain for \hat{n}_i , which is the particle occupation operator of the energy state, corresponding to energy level E_i :

$$\langle \hat{n}_i \rangle = \frac{1}{e^{\beta(E_i - \mu)} + 1} \equiv f(E_i, \mu) \quad (16)$$

where f is the Fermi function.

4 Greenfunctions

4.1 Equilibrium Greenfunctions

In the following we work in the Heisenberg picture, therefore the Schrödinger equation turns into:

$$i\hbar\dot{A} = [A, \hat{H}] \quad (17)$$

where \hat{H} is the Hamilton operator

We define the time-ordered Greenfunktion $G_{AB}^t(t, t')$ to be:

$$G_{AB}^t(t, t') = -i\langle T\{A(t)B(t')\} \rangle \quad (18)$$

where T is the time ordering operator, defined as

$$T\{A(t)B(t')\} = \Theta(t - t')A(t)B(t') - \Theta(t' - t)B(t')A(t) \quad (19)$$

with the Heavyside step function: $\Theta(x) = \begin{cases} 1 & x > 0 \\ 0 & x < 0 \end{cases}$

We further define four other Greenfunctions, the retarded and advanced

$$G_{AB}^r(t, t') = -i\Theta(t - t')\langle \{A(t), B(t')\} \rangle \quad (20)$$

$$G_{AB}^a(t, t') = i\Theta(t' - t)\langle \{A(t), B(t')\} \rangle \quad (21)$$

and the greater and lesser Greenfunctions:

$$G_{AB}^<(t, t') = i\langle B(t')A(t) \rangle \quad (22)$$

$$G_{AB}^>(t, t') = -i\langle A(t)B(t') \rangle \quad (23)$$

In equilibrium, all Greenfunctions have the property:

$$G_{AB}^\alpha(t, t') = G_{AB}^\alpha(t - t') \quad (24)$$

where $\alpha \in \{t, r, a, <, >\}$

The Greenfunctions follow the equations of motion:

$$i\hbar \frac{d}{dt} G_{AB}^\alpha(t, t') = \hbar \delta(t - t') \langle \{A(0), B(0)\} \rangle + G_{[A, \hat{H}]B}^\alpha(t, t') \quad (25)$$

with $\alpha \in \{t, r, a\}$

$$i\hbar \frac{d}{dt} G_{AB}^\alpha(t, t') = G_{[A, \hat{H}]B}^\alpha(t, t') \quad (26)$$

with $\alpha \in \{<, >\}$

4.2 Fourier transformation

We will use the following conventions for Fourier transformations between time t and energy E .

$$t \rightarrow E : \quad f(E) = \int_{-\infty}^{+\infty} dt f(t) e^{\frac{i}{\hbar} E t} \quad (27)$$

$$E \rightarrow t : \quad f(t) = \frac{1}{2\pi\hbar} \int_{-\infty}^{+\infty} dE f(E) e^{-\frac{i}{\hbar} E t} \quad (28)$$

For the delta function, we have the important identities:

$$\delta(E - E') = \frac{1}{2\pi\hbar} \int_{-\infty}^{+\infty} dt e^{-\frac{i}{\hbar}(E-E')t} \quad (29)$$

$$\delta(t - t') = \frac{1}{2\pi\hbar} \int_{-\infty}^{+\infty} dE e^{\frac{i}{\hbar} E(t-t')} \quad (30)$$

4.3 Example

For example, we assume a system of N noninteracting electrons, with discrete energy levels ϵ_k . We compute the retarded, advanced and lesser Greenfunctions for the operators $A = c_k$ and $B = c_k^\dagger$, which will later be needed.

Given Eq. (14), our non-interacting model Hamiltonian can be written as:

$$\hat{H} = \sum_k \epsilon_k c_k^\dagger c_k \quad (31)$$

Using (26) for the lesser Greens function

$$g_k^<(t, t') \equiv i \langle c_k^\dagger(t') c_k(t) \rangle \quad (32)$$

one needs to compute the commutator:

$$[c_k, \hat{H}] = \sum_i \epsilon_i [c_k, c_i^\dagger c_i] \stackrel{(10)}{=} \epsilon_k c_k \quad (33)$$

Therefore we obtain:

$$i\hbar \frac{d}{dt} g_k^<(t, t') = \epsilon_k g_k^<(t, t') \quad (34)$$

Hence using Eq. (24):

$$i\hbar \frac{d}{d(t-t')} g_k^<(t-t') = \epsilon_k g_k^<(t-t') \quad (35)$$

Solving the differential equation, we obtain:

$$g_k^<(t-t') = g_k^<(t=t') e^{-\frac{i}{\hbar} \epsilon_k (t-t')} = i \langle c_k^\dagger(0) c_k(0) \rangle e^{-\frac{i}{\hbar} \epsilon_k (t-t')} \stackrel{(9)}{=} i \langle \hat{n}_k \rangle e^{-\frac{i}{\hbar} \epsilon_k (t-t')} \quad (36)$$

Therefore our solution is (using (6)):

$$g_k^<(t-t') = i f(\epsilon_k, \mu) e^{-\frac{i}{\hbar} \epsilon_k (t-t')} \quad (37)$$

Now compute the advanced and the retarded Greenfunctions:

$$i\hbar \frac{d}{dt} g_k^{r,a}(t, t') = \hbar \delta(t-t') + \epsilon_k g_k^{r,a}(t, t') \quad (38)$$

Fourier transforming the equation $(t-t') \rightarrow E$ yields:

$$E g_k^{r,a}(E) = \hbar + \epsilon_k g_k^{r,a}(E) \quad (39)$$

Hence,

$$g_k^{r,a}(E) = \frac{\hbar}{E - \epsilon_k \pm i0^+} \quad (40)$$

where the usual term $\pm i0^+$ with $0^+ \in \mathbb{R}^+$ and 0^+ infinitesimal has been added, to suit the initial conditions. Integrating over residues, yields the Greenfunctions:

$$g_k^{r,a}(t, t') = \mp i \Theta(\pm t \mp t') e^{-\frac{i}{\hbar} \epsilon_k (t-t')} \quad (41)$$

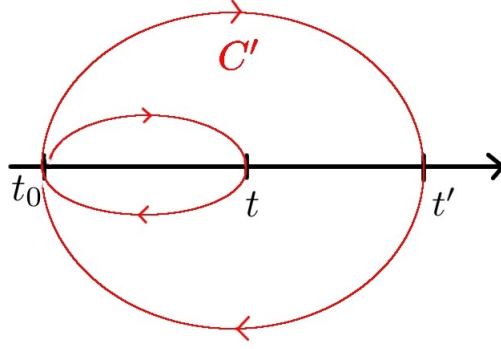


Figure 3: Contour C'

4.4 Nonequilibrium Greenfunctions

We assume that our system is a nonequilibrium at time $t > t_0$ while for $t < t_0$ the system had been in equilibrium.

Due to the Keyldish formalism evolving our nonequilibrium system out of an equilibrium system is mathematically equal to an equilibrium theory on special complex contours.

So we define nonequilibrium Greenfunctions, which are not dependent on t and t' with $t, t' \in \mathbb{R}$, but on τ^3 and τ' , with $\tau, \tau' \in C'$ (see figure 3).

The analogue of the time-ordered Greenfunction, called the contour-ordered Greenfunction $G_{AB}^c(t, t')$ has the form:

$$G_{AB}^c(t, t') = -i \langle T_{C'} \{A(t)B(t')\} \rangle \quad (42)$$

where $T_{C'}$ is the time ordering operator on the contour C' .

All other nonequilibrium Greenfunctions can be now defined analogue to the equilibrium ones, but on the new timecontour.

To compute the nonequilibrium Greenfunctions we use the Langreth theorem. If we start with:

$$G_{AB}^c(t, t') = \int_{C'} d\tau E^c(t, \tau) F^c(\tau, t') \quad (43)$$

where E^c, F^c are some arbitrary contour-ordered Greenfunctions, the Langreth theorem tells us that we can write:

$$G_{AB}^{<,neq}(t, t') = \int_{-\infty}^{+\infty} d\tilde{t} [E^r(t, \tilde{t}) F^<(\tilde{t}, t') + E^<(t, \tilde{t}) F^a(\tilde{t}, t')] \quad (44)$$

³We use greek letters for complex times and arabic letters for real times.

where $G_{AB}^{<,neq}$ is the nonequilibrium lesser Greenfunction.

Part II

Current through a quantum dot coupled to leads: Theoretical approach

5 Assumptions

- Both leads have discrete energy levels ϵ_k ($k \in \{k_{left}, k_{right}\}$).
- For simplicity we further assume, that the electrons in our leads are noninteracting
- To get a nonequilibrium situation, we assume that $\mu_l > \mu_r$, where μ_l is the chemical potential in the left and μ_r is the chemical potential in the right lead (see figure 2 for $T = 0$).
- Our quantumdot has only one energy level ϵ_d .
- Electrons of both leads are able to hop back and forth between quantum dot and lead, but as the leads are already in diagonal representation, there are no hops within the leads.

6 Base and Hamiltonian

The Hamilton operator of our whole system can be written as:

$$\hat{H} = \hat{H}_{w.h.} + \hat{H}_h \quad (45)$$

where $\hat{H}_{w.h.}$ describes the two leads and the quantumdot, but not the hopping between them. Hence:

$$\hat{H}_{w.h.} = \hat{H}_{left} + \hat{H}_{dot} + \hat{H}_{right} \quad (46)$$

As the electrons of our system can only be described by the energy level they occupy, the eigenvalues of the operator $\hat{H}_{w.h.}$ are equivalent to combinations of these energy levels.

Now we span our Hilbert space by the ONB \mathcal{B} , which consists of the eigenvectors of $\hat{H}_{w.h.}$ (according to equation (2)):

$$\mathcal{B} = \{|N; n_{k_1} n_{k_2} \dots\rangle\} \quad (47)$$

where $k_i \in \{k_{left}, k_d, k_{right}\}$

According to equation (14), $\hat{H}_{w.h.}$ turns into :

$$\hat{H}_{w.h.} = \sum_{k \in \{k_{left}\}} \epsilon_k c_k^\dagger c_k + \epsilon_d d^\dagger d + \sum_{k \in \{k_{right}\}} \epsilon_k c_k^\dagger c_k \quad (48)$$

Again using equation (14), we write \hat{H}_h in the second quantization form :

$$\hat{H}_h = \sum_{k_1, k_2} \langle \varphi_{k_1} | \hat{H}_{h., op} | \varphi_{k_2} \rangle c_{k_1}^\dagger c_{k_2} \quad (49)$$

where $|\varphi_{k_i}\rangle$ is the single particle state of an electron with energy ϵ_{k_i} and $\hat{H}_{h., op}$ is the single particle hopping operator.

Defining

$$\langle \varphi_{k_i} | \hat{H}_{h., op} | \varphi_{k_d} \rangle \equiv V_{k_i} \quad (50)$$

and using the assumptions of the last subsection, we get:

$$\hat{H}_h = \sum_{k \in \{k_{left}, k_{right}\}} \left(V_k c_k^\dagger d + V_k^* d^\dagger c_k \right) \quad (51)$$

Hence the total Hamiltonian has the form:

$$\hat{H} = \sum_{k \in \{k_{left}, k_{right}\}} \epsilon_k c_k^\dagger c_k + \epsilon_d d^\dagger d + \sum_{k \in \{k_{left}, k_{right}\}} \left(V_k c_k^\dagger d + V_k^* d^\dagger c_k \right) \quad (52)$$

This can also be written in the compact general form:

$$\hat{H} = \sum_{k_1, k_2} H_{k_1 k_2} c_{k_1}^\dagger c_{k_2} \quad (53)$$

7 Current I

We write the current I_l , which is the current from the left to the right lead, as:

$$I_l = -e \langle \dot{N}_l \rangle_{neq} \quad (54)$$

where $N_l = \sum_{k \in \{k_{left}\}} n_k$ is the particle number operator of the left lead. In our case we can think

of applying the Keyldish formalism in the following way:

At t_0 (we choose $t_0 = -\infty$) the two leads and the quantum dot are decoupled ($\Rightarrow \hat{H} = \hat{H}_{w.h.}$) and separately in equilibrium, while at time t , \hat{H}_h is fully activated.

Now we start computing:

$$I_l \stackrel{(17)}{=} \frac{ie}{\hbar} \langle [N_l, \hat{H}] \rangle_{neq} = \frac{ie}{\hbar} \sum_{k \in \{k_{left}\}} \langle [c_k^\dagger c_k, \hat{H}] \rangle_{neq} \quad (55)$$

using (53) yields:

$$I_l = \frac{ie}{\hbar} \sum_{k_1, k_2} \sum_{k \in \{k_{left}\}} \langle [c_k^\dagger c_k, H_{k_1 k_2} c_{k_1}^\dagger c_{k_2}] \rangle_{neq} \stackrel{(11)}{=} \frac{ie}{\hbar} \sum_{k \in \{k_{left}\}} \left(V_k \langle c_k^\dagger d \rangle_{neq} - V_k^* \langle d^\dagger c_k \rangle_{neq} \right) \quad (56)$$

Now we define:

$$G_k^{<,neq}(t, t') = i \langle c_k^\dagger(t') d(t) \rangle_{neq} \quad (57)$$

And therefore write (56) as:

$$I_l = \frac{2e}{\hbar} \sum_{k \in \{k_{left}\}} Re \{ V_k G_k^{<,neq}(t, t) \} \quad (58)$$

First we try to get an expression for the time-ordered Greenfunction $G_k^t(t, t')$ ⁴.

The equation of motion (25) for t' yields:

$$i\hbar \frac{d}{dt'} G_k^t(t, t') = -\hbar \delta(t - t') \langle \{d(0), c_k^\dagger(0)\} \rangle - i \langle T \{d(t) [c_k^\dagger(t'), \hat{H}] \} \rangle \quad (59)$$

Computing the commutator and defining:

$$G_d^t(t, t') = -i \langle T \{d(t) d^\dagger(t')\} \rangle \quad (60)$$

we obtain:

$$\left(-i\hbar \frac{d}{dt'} - \epsilon_k \right) G_k^t(t, t') = V_k^* G_d^t(t, t') \quad (61)$$

fourier transforming (61) from $(t - t')$ to E , we get:

$$(E - \epsilon_k) G_k^t(E) = V_k^* G_d^t(E) \quad (62)$$

comparing with the derivation of (40), we recognize⁵

$$G_k^t(E) = \frac{V_k^*}{\hbar} G_d^t(E) g_k^\alpha(E) \quad (63)$$

⁴As we can get $G_k^c(t, t')$ by changing the timeset for the time-ordered Greenfunction $G_k^t(t, t')$.

⁵We can use the results of subsection 4.3, as $\mathcal{H}_{w.h.}$ has the same form, as in the there used model Hamiltonian.

with $\alpha = r, a, t$ ⁶. But now, the left hand side of (63) and $G_d^t(E)$ have an equal number of poles in the upper and in the lower complex halfplane, as they are both time-ordered Greenfunctions. Therefore α has to be equal to t , too.

$$G_k^t(E) = \frac{V_k^*}{\hbar} G_d^t(E) g_k^t(E) \quad (64)$$

Using the convolution theorem yields:

$$G_k^t(t, t') = -\frac{V_k^*}{\hbar} \int_{-\infty}^{+\infty} d\tilde{t} G_d^t(t, \tilde{t}) g_k^t(\tilde{t}, t') \quad (65)$$

Now we switch to nonequilibrium by changing the integration set from \mathbb{R} to C'

$$G_k^c(t, t') = -\frac{V_k^*}{\hbar} \int_{C'} d\tilde{\tau} G_d^c(t, \tilde{\tau}) g_k^c(\tilde{\tau}, t') \quad (66)$$

Applying the Langreth theorem yields:

$$G_k^{<,neq}(t, t') = -\frac{V_k^*}{\hbar} \int_{-\infty}^{+\infty} d\tilde{t} [G_d^r(t, \tilde{t}) g_k^<(\tilde{t}, t') + G_d^<(t, \tilde{t}) g_k^a(\tilde{t}, t')] \quad (67)$$

or:

$$G_k^{<,neq}(E) = \frac{V_k^*}{\hbar} [G_d^r(E) g_k^<(E) + G_d^<(E) g_k^a(E)] \quad (68)$$

If we now plug (68) in the fourier transformed equation (58) we obtain:

$$I_l = \frac{2e}{\hbar} \int_{-\infty}^{\infty} \frac{dE}{2\pi\hbar} \sum_{k \in \{k_{l_{eft}}\}} \frac{|V_k|^2}{\hbar} \text{Re} \{G_d^r(E) g_k^<(E) + G_d^<(E) g_k^a(E)\} \quad (69)$$

7.1 Continuum

When we assume the leads to be macroscopic in comparism with the dot, we can apply the continuum limit in replacing:

⁶As these Greenfunctions obey the same equation of motion.

$$\sum_{k \in \{k_{left}\}} \quad \text{by} \quad \int_{-\infty}^{\infty} d\epsilon \rho_l(\epsilon) \quad (70)$$

where $\rho_l(\epsilon)$ is the density of states in the left lead.

Transforming (69) to continuum yields:

$$I_l = \frac{2e}{\hbar} \int_{-\infty}^{\infty} \frac{dE}{2\pi\hbar} \int_{-\infty}^{\infty} d\epsilon \rho_l(\epsilon) \frac{|V_l(\epsilon)|^2}{\hbar} \text{Re} \{ G_d^r(E) g_l^<(E, \epsilon) + G_d^<(E) g_l^a(E, \epsilon) \} \quad (71)$$

Now we can obtain $g_l^<(E, \epsilon)$ and $g_l^a(E, \epsilon)$ by fourier transforming the continuumlimes of our results in (37) and (41):

$$g_l^<(E, \epsilon) = 2\pi\hbar i f(\epsilon, \mu_l) \delta(E - \epsilon) \quad (72)$$

$$g_l^a(E, \epsilon) = \pi\hbar i \delta(E - \epsilon) \quad (73)$$

Plugging (72) and (73) into (71) we get:

$$I_l = \frac{2e}{\hbar} \int_{-\infty}^{\infty} \frac{dE}{2\pi\hbar} \int_{-\infty}^{\infty} d\epsilon \rho_l(\epsilon) \frac{|V_l(\epsilon)|^2}{\hbar} 2\pi\hbar \text{Re} \left\{ i(G_d^r(E) f(\epsilon, \mu_l) \delta(E - \epsilon) + \frac{1}{2} G_d^<(E) \delta(E - \epsilon)) \right\} \quad (74)$$

Integrating over ϵ , using $\text{Re}\{iz\} = -\text{Im}\{z\}$ and defining the hybridization function for the left lead $\Gamma_l(E)$, with:

$$\Gamma_l(E) = 2\pi\rho_l(E)|V_l(E)|^2 \quad (75)$$

yields:

$$I_l = -\frac{2e}{\hbar} \int_{-\infty}^{\infty} \frac{dE}{2\pi\hbar} \Gamma_l(E) \text{Im} \left\{ G_d^r(E) f_l(E) + \frac{1}{2} G_d^<(E) \right\} \quad (76)$$

where we defined $f_l(E) \equiv f(E, \mu_l)$ for simplicity

7.2 Symmetrization of the current

We can write the current I from left to right in the symmetrized form:

$$I = \frac{1}{2}(I_l - I_r) \quad (77)$$

where I_r is the current from right to left.

By using (76) we attain the symmetrized current:

$$I = -\frac{e}{\hbar} \int_{-\infty}^{\infty} \frac{dE}{2\pi\hbar} \text{Im} \left\{ G_d^r(E) (f_l(E)\Gamma_l(E) - f_r(E)\Gamma_r(E)) + \frac{1}{2}G_d^<(E) (\Gamma_l(E) - \Gamma_r(E)) \right\} \quad (78)$$

Now, to obtain our final result, we have to compute the equilibrium Greenfunctions $G_d^r(E)$ and $G_d^<(E)$.

7.3 Computation of $G_d^r(E)$

According to (20), $G_d^r(t, t')$ is defined as:

$$G_d^r(t, t') = -i\Theta(t - t') \langle \{d(t), d^\dagger(t')\} \rangle \quad (79)$$

Using the equation of motion in (25) for t' , computing the occuring commutator and fourier transforming the equation, we achieve:

$$(E - \epsilon_d)G_d^r(E) = \hbar + \sum_{k \in \{k_{left}, k_{right}\}} V_k G_k^r(E) \quad (80)$$

Now we need to know $G_k^r(E)$. When we write the fourier transformed equation of motion in (62) for $G_k^r(E)$, we get:

$$(E - \epsilon_k)G_k^r(E) = V_k^* G_d^r(E) \quad (81)$$

Analogue to the discussion done to get from (62) to (64) we can write (81) as:

$$G_k^r(E) = \frac{V_k^*}{\hbar} G_d^r(E) g_k^r(E) \quad (82)$$

and obbey:

$$(E - \epsilon_d - \Sigma_d^r(E)) G_d^r(E) = \hbar \quad (83)$$

where we defined the retarded selfenergy $\Sigma_d^r(E)$ as:

$$\Sigma_d^r(E) = \sum_{k \in \{k_{left}, k_{right}\}} \frac{|V_k|^2}{\hbar} g_k^r(E) \quad (84)$$

When we then apply the continuum limit to $\Sigma_d^r(E)$ we get:

$$\Sigma_d^r(E) = \int_{-\infty}^{\infty} d\epsilon \rho_l(\epsilon) \frac{|V_l(\epsilon)|^2}{\hbar} g_l^r(E, \epsilon) + \int_{-\infty}^{\infty} d\epsilon \rho_r(\epsilon) \frac{|V_r(\epsilon)|^2}{\hbar} g_r^r(E, \epsilon) \quad (85)$$

And using:

$$g_{l/r}^r(E, \epsilon) = -\pi \hbar i \delta(E - \epsilon) \quad (86)$$

we attain:

$$\Sigma_d^r(E) = -\frac{i}{2}(\Gamma_l(E) + \Gamma_r(E)) \equiv -i\Gamma(E) \quad (87)$$

where we again used the definition of the hybridization function $\Gamma_{l,r}$ given in (75).

Therefore we completely computed $G_d^r(E)$ as:

$$G_d^r(E) = \frac{\hbar}{E - \epsilon_d + i\Gamma(E)} \quad (88)$$

7.4 Computation of $G_d^<(E)$

When we now want to repeat the last subsection for $G_d^<(E)$, with the equation of motion for the lesser Greenfunction (see (26)), we attain:

$$(E - \epsilon_d - \Sigma_d^<(E))G_d^<(E) = 0 \quad (89)$$

Because of the zero on the right side we won't be successful following the same way as in the last subsection. We solve the problem by using the (general) Keyldish-equation for a noninteracting system:

$$G^<(E) = \frac{1}{\hbar} G^r(E) \Sigma^<(E) G^a(E) \quad (90)$$

To get $\Sigma_d^<(E)$, in analogy to (84), we write:

$$\Sigma_d^<(E) = \sum_{k \in \{k_{left}, k_{right}\}} \frac{|V_k|^2}{\hbar} g_k^<(E) \quad (91)$$

again doing the continuum limit and using (72) for $g_{l/r}^<(E)$ yields:

$$\Sigma_d^<(E) = i(f_l(E)\Gamma_l(E) + f_r(E)\Gamma_r(E)) \quad (92)$$

To get $G_d^a(E)$ we only have to change the sign of the Selfenergy in (88):

$$G_d^a(E) = \frac{\hbar}{E - \epsilon_d - i\Gamma(E)} \quad (93)$$

So using the Keyldish equation, we attain:

$$G_d^<(E) = i \frac{\hbar(f_l(E)\Gamma_l(E) + f_r(E)\Gamma_r(E))}{(E - \epsilon_d)^2 + \Gamma^2(E)} \quad (94)$$

7.5 Final Result

We can write this equation the following way:

$$I = -\frac{e}{\hbar} \int_{-\infty}^{\infty} \frac{dE}{2\pi\hbar} \left(\text{Im}\{G_d^r(E)\} (f_l(E)\Gamma_l(E) - f_r(E)\Gamma_r(E)) + \frac{1}{2} \text{Im}\{G_d^<(E)\} (\Gamma_l(E) - \Gamma_r(E)) \right) \quad (95)$$

With (88) we can compute $\text{Im}\{G_d^r(E)\}$:

$$\text{Im}\{G_d^r(E)\} = \text{Im} \left\{ \frac{\hbar}{E - \epsilon_d + i\Gamma(E)} \right\} = -\frac{\hbar}{2} \frac{\Gamma_l(E) + \Gamma_r(E)}{(E - \epsilon_d)^2 + \Gamma^2(E)} \quad (96)$$

And with (94) we can immediately compute $\text{Im}\{G_d^<(E)\}$:

$$\text{Im}\{G_d^<(E)\} = \frac{\hbar(f_l(E)\Gamma_l(E) + f_r(E)\Gamma_r(E))}{(E - \epsilon_d)^2 + \Gamma^2(E)} \quad (97)$$

putting these expressions in (95) we achieve the final result:

$$I = \frac{e}{\hbar} \int_{-\infty}^{\infty} dE \frac{\Gamma_l(E)\Gamma_r(E)}{(E - \epsilon_d)^2 + \Gamma^2(E)} (f_l(E) - f_r(E)) \quad (98)$$

7.6 Discussion of the result for $T=0$

As our simulation also will be done at Temperature $T = 0$, we will now discuss our result in this limit. Because of the Fermi functions becoming stepfunctions in the $T = 0$ limes, the difference of Fermi functions $f_l - f_r$, emerging in our result, gets:

$$f_l - f_r = \begin{cases} 1 & \mu_r < E < \mu_l \\ 0 & \text{otherwise} \end{cases} \quad (99)$$

Therefore (98) becomes:

$$I = \frac{e}{h} \int_{\mu_r}^{\mu_l} dE \frac{\Gamma_l(E)\Gamma_r(E)}{(E - \epsilon_d)^2 + \Gamma^2(E)} \quad (100)$$

At this point we need to discuss the hybridization functions $\Gamma_{l,r}$ in (75):

$$\Gamma_{l/r}(E) = 2\pi\rho_{l/r}(E)|V_{l/r}(E)|^2 \quad (101)$$

Due to the definition of the V_k 's, their squared modulus is a measure for the probability of one electron to hop from the d-level to the k-level (or vice versa as $|V_k|^2 = |V_k^*|^2$). When we hence multiply $|V_{l/r}(E)|^2$ with the density of states in the left/right lead $\rho_{l/r}(E)$, we get the probability density of electrons moving from the d-level to the left/right lead at energy E and $\Gamma_{l,r}$ being proportional to that probability-density.

Now we assume that the hybridization functions no longer depend of E , as every lead-electron should have the same possibility for tunneling no matter which energy the electron has. Further we assume that the leads are identical, which means:

$$\Gamma_l = \Gamma_r = \Gamma \quad (102)$$

Now we can write (100) as:

$$I = \frac{e}{h} \int_{\mu_r}^{\mu_l} dE \Gamma \frac{1}{(E - \epsilon_d)^2 + \Gamma^2} \Gamma \quad (103)$$

Besides of a norming constant, the Lorentzian $L(E, \epsilon_d, \Gamma)$ in (103) (compare figure 4):

$$L(E, \epsilon_d, \Gamma) = \frac{1}{(E - \epsilon_d)^2 + \Gamma^2} \quad (104)$$

⁷In our derivation we assumed that $E \in] - \infty, \infty[$, but introducing a lower band edge D , which is equal for both leads yields the same result

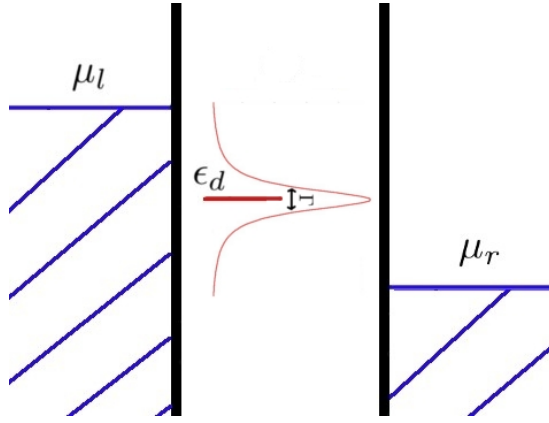


Figure 4: System and Lorentzian $L(E, \epsilon_d, \Gamma)$ plotted in energyspace

describes the possibility density of an electron located at energy level ϵ_d to have an energy E , which follows from the fact, that the electron leaves this level in the characteristic time τ . Because of that we obtain two new properties of Γ :

- Γ represents the inverse lifetime τ of an electron on the d-level,

$$\Gamma = \frac{\hbar}{\tau} \quad (105)$$

- Γ represents the FWHM (full width half maximum) of $L(E, \epsilon_d, \Gamma)$.

Using this considerations, we can interpret equation (103). We get the whole current, by integrating the propability density of electrons to pass from left to right with energy E . This density consists of the propability of moving from left to d (Γ), the propability for having energy E in d ($\frac{1}{(E-\epsilon_d)^2+\Gamma^2}$) and the propability to get from d to right (Γ).

At the end of this section, we solve (103) for a symmetrized case. We let $\epsilon_d = 0$ and

$$\mu_l = -\mu_r \equiv \frac{eV}{2} \quad (106)$$

where V is the electrical potential. Hence (103) turns into:

$$I = \frac{e}{h} \int_{-\frac{eV}{2}}^{\frac{eV}{2}} dE \frac{\Gamma^2}{E^2 + \Gamma^2} \quad (107)$$

And we derive the expression:

$$I(V) = \frac{2e\Gamma}{h} \arctan\left(\frac{eV}{2\Gamma}\right) \quad (108)$$

Now we can discuss the behavior of the achieved result for the $eV \ll \Gamma$ regime:

As the argument of the arcustangens then gets $\ll 1$, we taylor expand $I(V)$:

$$I(V) = \frac{2e\Gamma}{h} \left(\frac{eV}{2\Gamma} \right) = \frac{e^2}{h} V \equiv \frac{G_0}{2} V \quad (109)$$

where we defined the conductance quantum

$$G_0 = \frac{2e^2}{h} \quad (110)$$

The factor 2 is due to our simplification, that we neglected the spin of our noninteracting electrons. Respecting the spin, every energy level can be occupied by two electrons and therefore we get two times our derived current.

7.7 Conductance Quantum

For ballistic transport through a single quantum channel, which is coupled to the electrical potential V , the current-potential dependency is given by:

$$I(V) = \frac{2e^2}{h} V \equiv G_0 V \quad (111)$$

When we consider equation (103) in the $eV \ll \Gamma$ regime, we can approximate the integrand by a constant function. And as the integrand is proportional to the propability to get from left to right at energy E , it stays normalized. That is why we get a δ -distribution at $E = 0$ when $eV \rightarrow 0$. This means, that we have only a single channel, the electron can pass and therefore we fullfill the conditions for ballistic transport.

Part III

Current through a quantum dot coupled to leads: Simulation

In this part we simulate the current through the quantum dot with gnu octave and then compare with (108). Our main problem will be, that we assumed the energy levels in the leads to be continuous. As we can't simulate continuous energy levels, we will have to discretize the leads. We will present two different discretizations.

8 Determining $I(t)$

Referring to (56), we were able to write the current I_l as:

$$I_l = -\frac{2e}{\hbar} \sum_{k \in \{k_{left}\}} \text{Im} \left\{ V_k \langle c_k^\dagger d \rangle_{neq} \right\} \quad (112)$$

with the expectation value $\langle \cdot \rangle_{neq}$ due to the Keyldish formalism.

Now using a numerical simulation for a noninteracting system, we can solve the Schrödinger equation for arbitrary times. Therefore we don't let $t_0 \rightarrow -\infty$, but rather take the initial state $|\psi\rangle$ (at time $t_0 = 0$), which consists of the occupied energy levels at the beginning (figure 2), and compute the current for the time evolved $|\psi(t)\rangle$. Because of that, we now get a time-dependent, not a steady state current. We also expect the current to show finite size effects, as we will reach the point, when we have more electrons in the right than in the left lead, which is due to the fact, that the effective V is no longer constant, but even changes sign with time.

Now we can pass to the Heisenberg picture by:

$$I_l(t) = \langle \psi(t) | \hat{I}_l | \psi(t) \rangle = \langle \psi | e^{\frac{i}{\hbar} \hat{H} t} \hat{I}_l e^{-\frac{i}{\hbar} \hat{H} t} | \psi \rangle \equiv \langle \psi | \hat{I}_l(t) | \psi \rangle \equiv \langle \hat{I}_l(t) \rangle \quad (113)$$

Therefore we replace $\langle \cdot \rangle_{neq}$ in (112) by $\langle \cdot \rangle$, as defined in (113) and get:

$$I_l(t) = -\frac{2e}{\hbar} \sum_{k \in \{k_{left}\}} Im \left\{ V_k \langle c_k^\dagger(t) d(t) \rangle \right\} \quad (114)$$

Now compute $c_k^\dagger(t)$ and $d(t)$ using (17):

$$i\hbar \frac{d}{dt} c_i(t) = [c_i, \hat{H}](t) \quad (115)$$

where $i \in \{k_{left}, k_{right}, k_d\}$

Using the matrix representation (see (53)) yields:

$$i\hbar \frac{d}{dt} c_i(t) = \sum_{j, k \in \{k_{left}, k_{right}, k_d\}} H_{jk} [c_i, c_j^\dagger c_k](t) \stackrel{(10)}{=} \sum_{k \in \{k_{left}, k_{right}, k_d\}} H_{ik} c_k(t) \quad (116)$$

Next we define the vector $\vec{c}(t)$, which is build of the annilation operators in the following way:

$$\vec{c}(t) = \begin{pmatrix} \vdots \\ c_i(t), i \in \{k_{left}\} \\ \vdots \\ c_{k_d}(t) \\ \vdots \\ c_i(t), i \in \{k_{right}\} \\ \vdots \end{pmatrix} \quad (117)$$

So (116) can be written as a matrix equation:

$$i\hbar \frac{d}{dt} \vec{c}(t) = H \vec{c}(t) \quad (118)$$

As \hat{H} is timeindependent, H is timeindependent, and therefore the linear differential equation can be solved by:

$$\vec{c}(t) = e^{-\frac{i}{\hbar} H t} \vec{c}(0) \equiv U(t) \vec{c}(0) \quad (119)$$

with the unitary matrix $U \equiv e^{-\frac{i}{\hbar} H t}$.

Now daggering both sides, we get a similar equation for $\vec{c}^\dagger(t)$:

$$\vec{c}^\dagger(t) = \vec{c}^\dagger(0) e^{\frac{i}{\hbar} H t} = \vec{c}^\dagger(0) U^\dagger(t) \quad (120)$$

where $\vec{c}^\dagger(t)$ is defined as:

$$\vec{c}^\dagger(t) = \left(\dots \quad c_i^\dagger(t), i \in \{k_{left}\} \quad \dots \quad c_{k_d}^\dagger \quad \dots \quad c_i^\dagger(t), i \in \{k_{right}\} \quad \dots \right) \quad (121)$$

Using these results, the expression for the current (114) turns into:

$$I_l(t) = -\frac{2e}{\hbar} \sum_{k \in \{k_{left}\}} \sum_{i,j \in \{k_{left}, k_{right}, k_d\}} \text{Im} \left\{ V_k U_{ik}^\dagger(t) U_{dj}(t) \langle c_i^\dagger c_j \rangle \right\} \quad (122)$$

where we denoted $c_i^\dagger(0) \equiv c_i^\dagger$ and $c_j(0) \equiv c_j$

Now

$$\langle c_i^\dagger c_j \rangle = \langle \psi | c_i^\dagger c_j | \psi \rangle = \delta_{ij} \langle \hat{n}_i \rangle \quad (123)$$

The last equality follows from the fact, that $|\psi\rangle = \prod_{i' \in \{k_{start}\}} c_{i'}^\dagger |0\rangle$ and from the fundamental anti-commutation relations of annihilation and creation operators (compare (7),(8)).

Because of that, the current formula (122) turns into:

$$I_l(t) = -\frac{2e}{\hbar} \sum_{k \in \{k_{left}\}} \sum_{i \in \{k_{start}\}} \text{Im} \left\{ V_k U_{di}(t) U_{ik}^\dagger(t) \right\} \quad (124)$$

Symmetrizing the current as in (77) yields:

$$I(t) = -\frac{e}{\hbar} \sum_{i \in \{k_{start}\}} \left(\sum_{k \in \{k_{left}\}} \text{Im} \left\{ V_k U_{di}(t) U_{ik}^\dagger(t) \right\} - \sum_{k \in \{k_{right}\}} \text{Im} \left\{ V_k U_{di}(t) U_{ik}^\dagger(t) \right\} \right) \quad (125)$$

The initial electrical potential V appears in the set, the first sum runs over. We can now write this equation in matrix product form:

$$I(t) = -\frac{e}{\hbar} \text{Im} \left\{ \vec{U}_d(t) \tilde{U}^\dagger(t) \vec{V}_{all} \right\} \quad (126)$$

where

- $\vec{U}_d = (U_{di} \mid i \in \{k_{start}\}) \in \mathbb{C}^{1 \times |\{k_{start}\}|}$,
- $\tilde{U}^\dagger = \left(U_{ik}^\dagger \mid i \in \{k_{start}\}, k \in \{k_{left}, k_{right}\} \right) \in \mathbb{C}^{|\{k_{start}\}| \times (|\{k_{left}\}| + |\{k_{right}\}|)}$
- and $\vec{V}_{all} = \begin{pmatrix} V_k \mid k \in \{k_{left}\} \\ -V_k \mid k \in \{k_{right}\} \end{pmatrix} \in \mathbb{C}^{(|\{k_{left}\}| + |\{k_{right}\}|) \times 1}$

The minus sign is due to the sign between the inner sums in (125).

8.1 Cleaning up with dimensions

Up to this point, we had been working with the natural constants \hbar and e . As we now want to simulate our system, we set:

$$\hbar = 1 \quad , \quad e = 1 \quad (127)$$

With the following effects:

- Setting $\hbar = 1$ means, choosing a time scale relevant for quantum mechanics, when absorbing the \hbar in t ($e^{-\frac{i}{\hbar}Ht} \rightarrow e^{-iHt}$).
- Setting $e = 1$ effects two quantities:
 - We measure the electrical potential in units of energy.
 - We measure the current not in charge per time, but in electrons per time.

Therefore the theoretical result (see (108)) turns into:

$$I(V) = \frac{\Gamma}{\pi} \arctan \left(\frac{V}{2\Gamma} \right) \quad (128)$$

And the equation used for the simulation (see (126)) turns into:

$$I(t) = -\text{Im} \left\{ \vec{U}_d(t) \tilde{U}^\dagger(t) \vec{V}_{all} \right\} \quad (129)$$

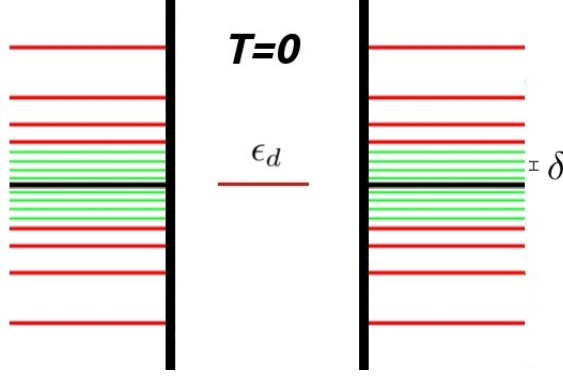


Figure 5: Linear discretization

for (left, right, d-level), respectively

Now we want to choose the energy levels in a way, that keeps us close to the continuum case, in which we developed (128).

We do several steps:

- Again we choose $\epsilon_d = 0$ and $\mu_l = -\mu_r = \frac{V}{2}$.
- For the linear discretization we want the two leads to have equal structure. Therefore we choose our ϵ_k 's to be equal on both sides and with the following symmetry

$$H_l = \begin{pmatrix} \epsilon_1 & & \\ & \ddots & \\ & & \epsilon_N \end{pmatrix} \text{ and } H_r = \begin{pmatrix} \epsilon_N & & \\ & \ddots & \\ & & \epsilon_1 \end{pmatrix} \quad (135)$$

where ϵ_1 is the lowest energyvalue, $\epsilon_N = -\epsilon_1$ the highest one.

- We choose $\epsilon_k \in [-1; 1]$ (bandwidth $D = 2$).
- As we are limited in the number of our energy levels to describe the full bandwidth and also want the most of our levels to be in the "interesting" interval $[-\frac{V}{2}; \frac{V}{2}]$, we choose a logarithmic discretezation for large energies, and a linear one within the window of the voltage bias (see Fig.5). The fact that the bandwidth in the theoretical approach had been ∞ is taken into account, when we choose the bandwidth D to be much larger then V . Hence we get our first bound:

$$V \ll D \quad (136)$$

As the single particle energy levels of each lead are choosen symmetric with respect to $E = 0$, we discuss e.g. the negative energy levels of the left lead. According to figure 6, we can write the ϵ_k^{low} 's as:

$$\epsilon_k^{low} = \begin{cases} -\Lambda^{-k+1} & k \in \{1, \dots, a\} \\ -\Lambda^{-a+1} + \delta k & k \in \{a+1, \dots, n\} \end{cases} \quad (137)$$



Figure 6: Discretization of the negative levels of the left lead

where the upper line corresponds to region (I) in figure 6, the lower line to region (II), and

- a is the number of exponential decaying levels in one lead above or below zero.
- n is the number of energy levels below or above zero in one lead.
- $N = 2n + 1$, where the $+1$ refers to the $\epsilon_k = 0$ energy level, as we want to choose the levels in the leads symmetrical around it.
- The uniform level spacing $\delta = \frac{\Lambda^{-a+1}}{n+1-a}$ is constructed the way that $0 - \epsilon_n^{low} = \epsilon_n^{low} - \epsilon_{n-1}^{low}$ (see Fig.5)

Now using the symmetry of the energy levels in one lead with respect to zero and (137), one gets the following energy levels:

$$\epsilon_k = \begin{cases} \epsilon_k^{low} & k \in \{1, \dots, n\} \\ 0 & k = n + 1 \\ -\epsilon_{N+1-k}^{low} & k \in \{n + 2, \dots, N\} \end{cases} \quad (138)$$

The ϵ_k constructed this way are illustrated in figure 7. The kink in the semilogarithmic plot is due to our special discretization. But this is no problem, since most happens in the linear discretized region. Furthermore we will also choose a constant the hybridization function Γ , which makes the simulation somewhat more insensitive to the exact details of the discretization.

9.1 Obtaining V_k

To use (126), we need to know the V_k 's. As defined in (75), we have:

$$\Gamma_l(E) = 2\pi\rho_l(E)|V_l(E)|^2 \quad (139)$$

and as defined in (102):

$$\Gamma = \frac{\Gamma_l + \Gamma_r}{2} \quad (140)$$

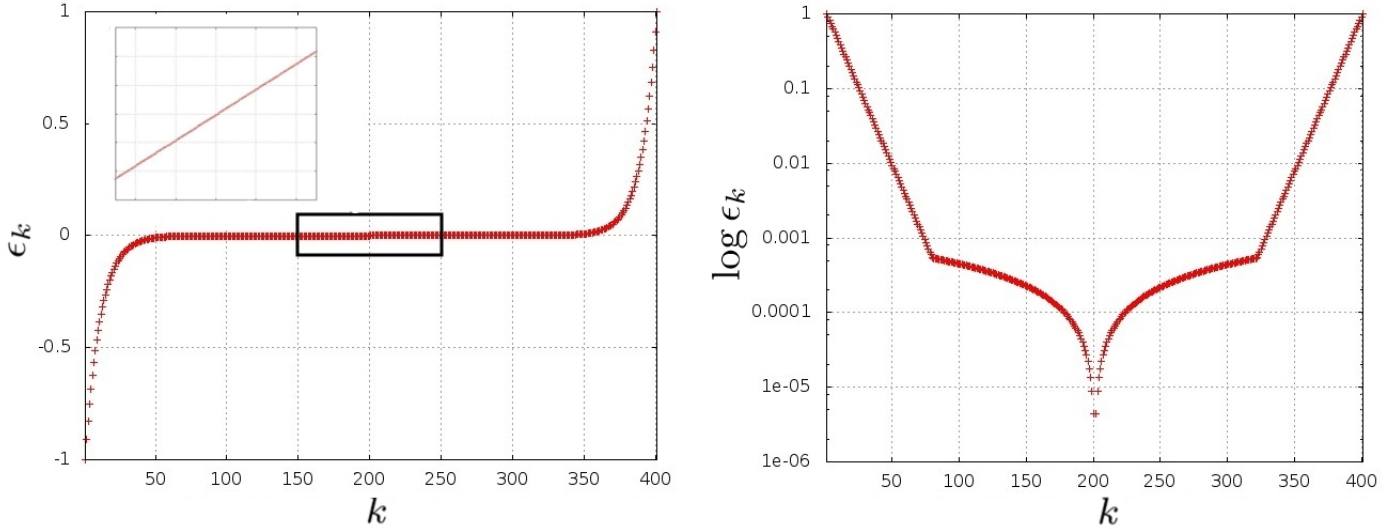


Figure 7: ϵ_k 's in normal and semilogarithmic plot

where we have chosen Γ to be constant again (see derivation of (108)).

Now we choose $\rho_l = \rho_r \equiv \rho$ and $V_l = V_r \equiv V$ as we want to have equal leads and go back to discrete k -values. Hence (139) turns into:

$$\Gamma = 2\pi\rho_k|V_k|^2 \quad (141)$$

Choose $V_k \in \mathbb{R}^\dagger$, we get an expression for the V_k 's:

$$V_k = \sqrt{\frac{\Gamma}{2\pi\rho_k}} \quad (142)$$

To compute V_k , we need the density of states ρ_k . In the discrete case we construct ρ_k in the following way. We set $\rho(\epsilon_k) \simeq \rho_k \equiv \frac{1}{\delta_k}$ (see figure 8), where δ_k specifies the average distance of level k to its nearest neighbor levels. This means, that we count one state per δ_k -interval. Choosing suitable boundary conditions, we obtain:

$$\rho_k = \begin{cases} \frac{1}{\epsilon_2 - \epsilon_1} & k = 1 \\ \frac{2}{\epsilon_{k+1} - \epsilon_{k-1}} & k \in \{2, \dots, N-1\} \\ \frac{1}{\epsilon_N - \epsilon_{N-1}} & k = N \end{cases} \quad (143)$$

9.2 Strategy of simulating $I(t)$

Now let's summarize the steps of the simulation:

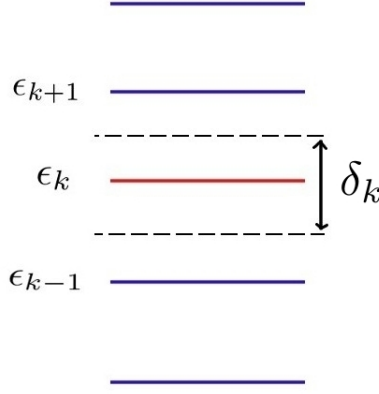


Figure 8: Constructing ρ_k

- First we have to build up our H -matrix, which has the dimension: $H \in \mathbb{R}^{M \times M}$. Here we can also choose a and Λ , when constructing the ϵ_k 's, and Γ , when constructing the V_k 's.
- Using the H -matrix, we can compute the unitary matrix U with

$$U(t) = e^{-iHt} = S e^{-iEt} S^\dagger \quad (144)$$

where $HS = SE$ diagonalizes the Hamiltonian

- Now, using (126) we can compute the current for different times, dependent on the electrical potential V .

9.3 Suggestive units

We can write our quantities in suggestive units.

For our time t we will consider two physical time scales:

- For short times we write t in units of $\tau = \frac{1}{\Gamma}$. This scale will be used, when we want to resolve processes like the transient behaviour of our current.
- For larger times we resolve the effects of discretization (finite size effects). Therefore we will choose the time unit T , which is the time, the system needs to show revival effects. As T is proportional to the number of energy levels our discretized system possesses, we have

$$T = \frac{2\pi}{\delta} \quad (145)$$

Because of that we obtain the second bound for two of our variables (the first one has been (136)), as one cannot see the long time behaviour, when $T \ll \tau$. This means:

$$T \gg \tau \leftrightarrow \Gamma \gg \delta \quad (146)$$

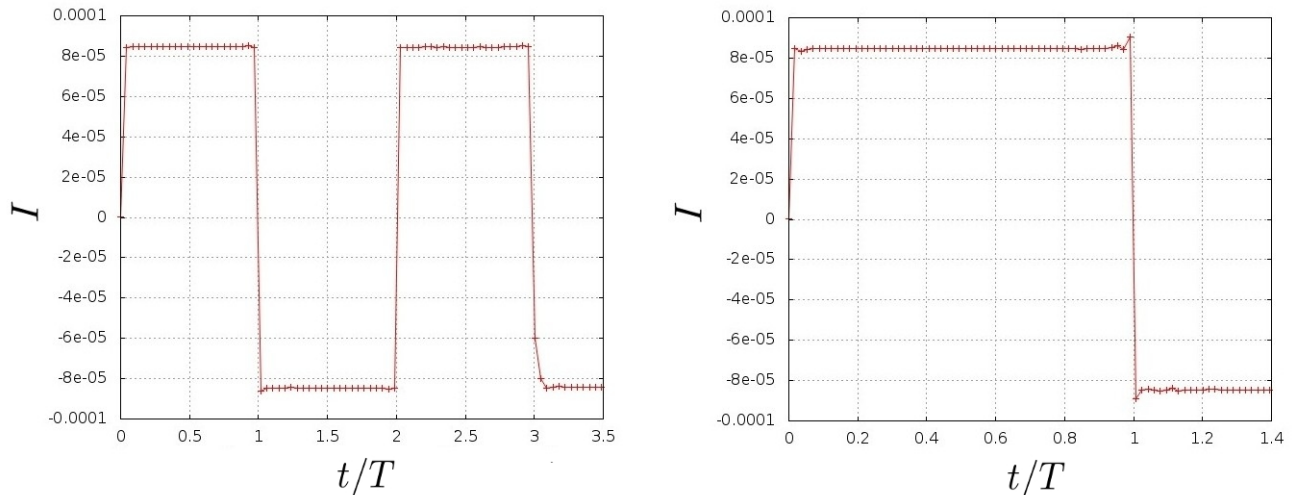


Figure 9: $I(t)$ for $V = 5.33e - 04(= 120\delta)$

Then we write the electrical potential V in units of Γ , which is independent of the discretization, resulting in a dimensionless quantity.

10 Results (linear discretization)

10.1 $I(t)$ -plots

The following results of time-dependent current $I(t)$ are based on the programs "H1matrix.m", "current1.m" and "tI1plot.m" (see appendix).

In figure 8 we used $M = 803$, $a = 80$, $\Lambda = 1.1$ and $\Gamma = 0.01$, (this implies $\delta = 4.438e - 06$). Discussing the left plot, we can see, that the current shows the deliberate bouncing behavior. In between, the current nearly adopts constant values. As we want to examine the steady state current from left to right (to be able to compare with (128)), we will take an average value of the first interval (see right plot), and use this value for the $I(V)$ -plot.

10.2 $I(V)$ -plots

The following uses program "IVplot.m" to attain a $I(V)$ -plot for our quantum dot coupled to the two leads.

To get the average steady state current $\langle I_s \rangle$ for particular electrical potential V , we take the average value of 40 datapoints located in the middle of our first interval in figure 8 ($t/T < 1$).

Now we want to compare our result with equation (128), which had been:

$$I(V) = \frac{\Gamma}{\pi} \arctan\left(\frac{V}{2\Gamma}\right) \quad (147)$$

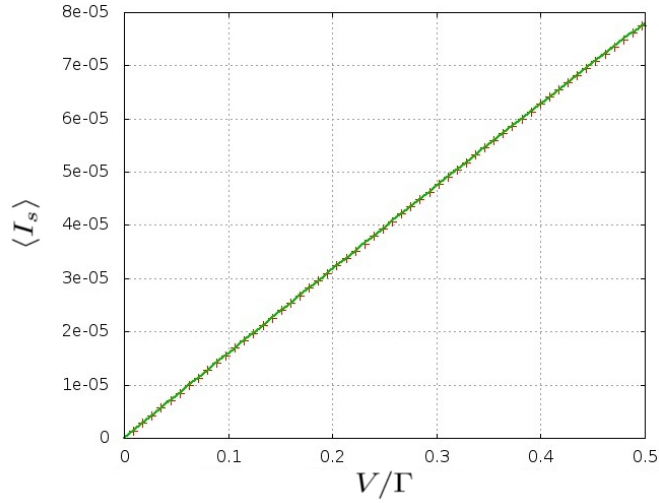


Figure 10: $\langle I_s \rangle(V)$ -plot for $\Gamma = 1e - 03$

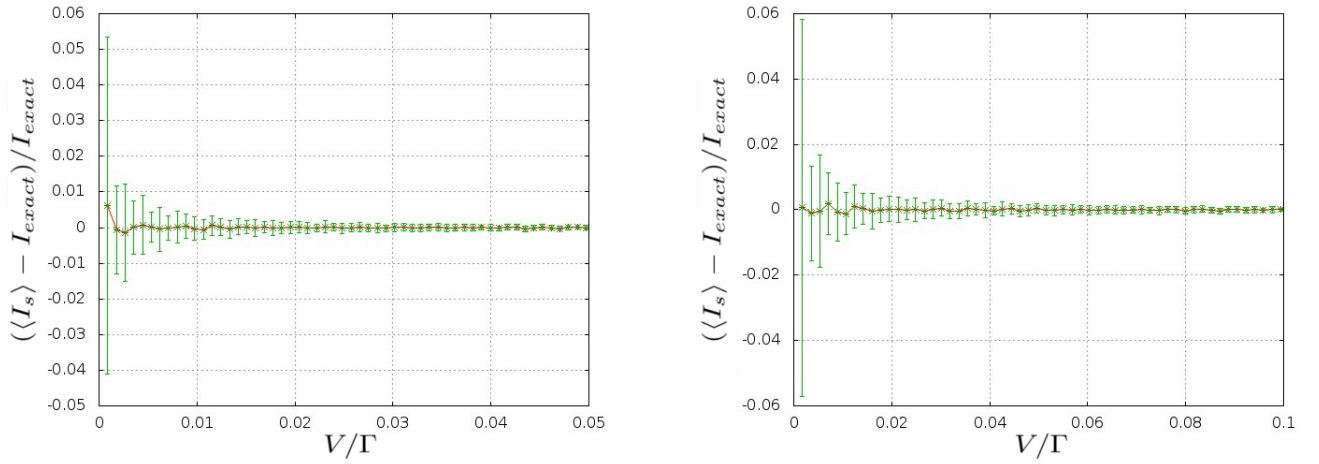


Figure 11: Absolute error of linear discretization for $\Gamma = 0.01$ and $\Gamma = 5e - 03$

In Fig.10, we can see the $\langle I_s \rangle(V)$ -plot for $\Gamma = 1e - 03$ illustrated with the exact theoretical result (solid green line). As there can't be seen any difference with the naked eye, we compute the relative error of the mean current values $((\langle I_s \rangle - I_{exact})/I_{exact})$ for different values of the electrical potential V , where I_{exact} is the theoretical result. In figure 11, we can see plots of the relative error for varying V (linked by red solid lines) with the error bars, one obtains when averaging the $I(t)$ -plots (also normed with I_{exact}). We recognize that the relative error stays quite small for both values of Γ and larger V/Γ -values. That the relative error attains its biggest values for small V/Γ -values is due to the fact, that I_{exact} gets really small while the absolute error stays nearly constant. One also recognizes that the perfect case ($I_{exact} - \langle I_s \rangle = 0$) lies in the error interval for all computed values of V and both Γ 's. By testing the match to the theoretical result, we also tested the absolute error in the conductance quantum behavior (for small V/Γ), discussed in

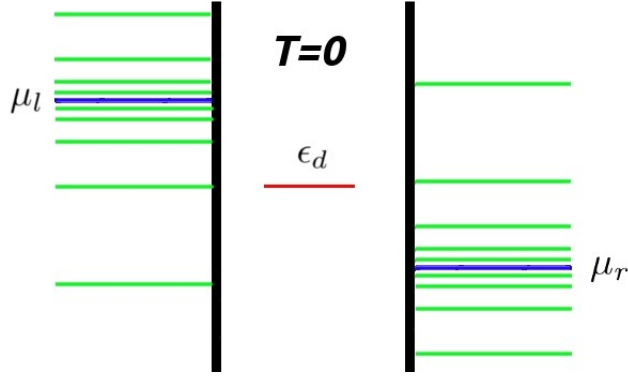


Figure 12: Pure logarithmic discretization relative to the chemical potential of each lead.

subsection 7.7. Because of the excellent agreement of the numerical data, obtained with linear discretization, to the theoretical result, we will use this discretization as a measure for the quality of the next discretization.

11 Logarithmic discretization

Now we want to use pure logarithmic discretization relative to our chemical potential. As $\mu_l \neq \mu_r$, the energy levels are no longer symmetrical in both leads, which is an important difference to the linear discretization. The discretization is visualised in figure 12. In the following we again choose $\epsilon_d = 0$ and $\mu_{l/r} = \pm \frac{U}{2}$.

One suspects, that this discretization will yield worse results than the first one, as a well resolved area in the left lead hits a badly resolved area in the right lead in terms of single particle levels and vice versa. Hence the current should be influenced by the discretization.

In the following we will use M , N , n and Λ as already introduced in section 8. We will also use the introduced suggestive units for our plots, except for the unit $\frac{2\pi}{\delta}$ for the larger timescale, as we do not have a constant level spacing in the logarithmic discretization case anymore.

11.1 Obtaining ϵ_k

We build our new ϵ_k 's in the following way. First we construct the logarithmic discretization around 0:

$$\tilde{\epsilon}_k = \begin{cases} -\Lambda^{-k+1} & k \in \{1, \dots, n\} \\ 0 & k = n + 1 \\ \Lambda^{k-N} & k \in \{n + 2, \dots, N\} \end{cases} \quad (148)$$

Then we translate the $\tilde{\epsilon}_k$'s and obtain:

$$\epsilon_k = \tilde{\epsilon}_k + \frac{U}{2} \quad k \in \{k_{left}\} \quad \epsilon_k = \tilde{\epsilon}_k - \frac{U}{2} \quad k \in \{k_{right}\} \quad (149)$$

11.2 Obtaining V_k

We have built the V_k 's with equation (142), which only depend on the ρ_k 's, besides of Γ , which we still choose to be constant. With equation (143), where the construction of the ρ_k 's is written down, we see that the ϵ_k 's only appear in terms as $\epsilon_{k+1} - \epsilon_k$, and hence the ρ_k 's (and also the V_k 's) can be constructed by using the $\tilde{\epsilon}_k$'s.

12 Results (logarithmic discretization)

12.1 $I(t)$ -plots

For the following results, we will still use $M = 803$ and $\Lambda = 1.1$ throughout.

Again we want to study two different regimes. The first is the longtime behaviour, which corresponds to the $I(t)$ -plots of the linear discretization, which had been in units of $\frac{2\pi}{\delta}$. In this time regime, one can resolve discretization effects. One can see the long time behavior in the left plots of the figures 13, 14 and 15, where the solid green line is the theoretical result obtained with Eq. (128). One can again see reflexion effects, as the current becomes negative. We also recognize, that the plots for larger values of Γ differ from the plot for $\Gamma = 1e - 03$, as they show more noise. What we also want to mention is, that the time T upon which the current turns negative, is approximately the same for our different plots, $T \simeq 2e05$. However, the plots are significantly more blurred as compared to the case of linear discretization.

The second regime we want to study is the short time behavior of the logarithmic discretization. For this purpose, let's look at the right plots of the figures 13, 14 and 15. Here we can see the transient behavior of our system and the theoretical value again. The plots show a similar behavior for all values of Γ and we also see, that the mean current values lie below the theoretically expected value.

As the longtime behavior of our logarithmic discretization does not behave as nicely as in the linear case, we choose the average interval, which we will use to attain $\langle I_s \rangle$ in the short-time regime as follows:

$$\Gamma t \in [5; 7] \tag{150}$$

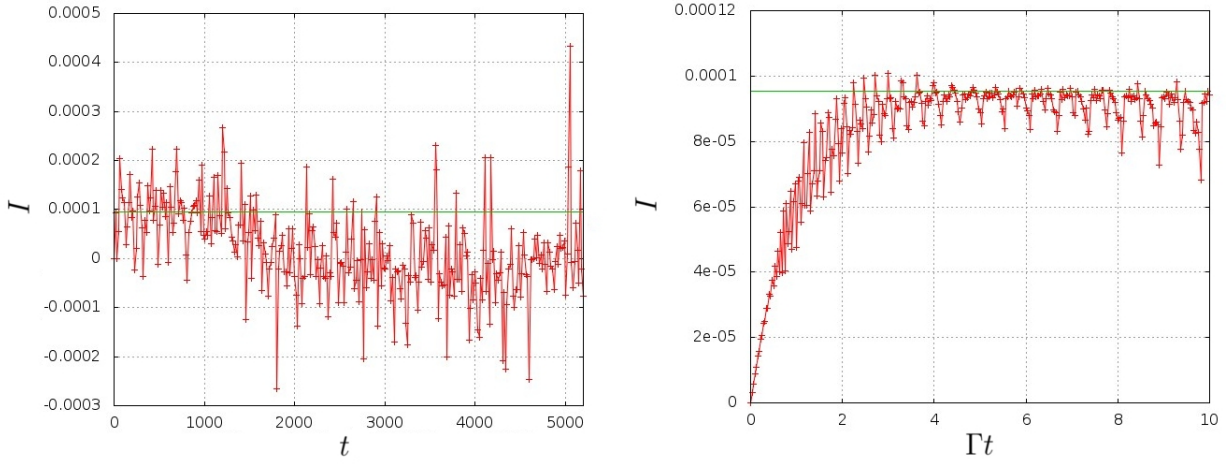


Figure 13: Long and short time regime for $\Gamma = 0.01$ and $V = 6e - 04$. The theoretical steady state current is indicated by the green horizontal line.

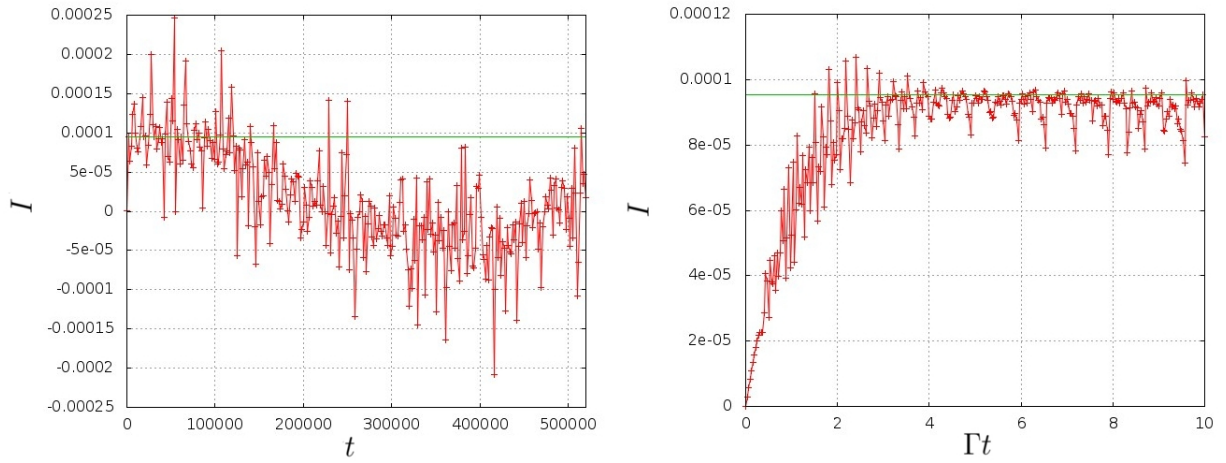


Figure 14: Long and short time plot for $\Gamma = 5e - 03$ (same as figure 13 otherwise)

12.2 $I(V)$ -plots

We construct the $I(V)$ - plots with the averaged values of our $I(t)$ -plots again, now using the interval [5; 7]. In Fig.16 one can see the $\langle I_s \rangle(V)$ -plot for $\Gamma = 1e - 03$. In comparison with figure 10, one can see the deviation of the numerical data to the theoretical result (solid green line) with the naked eye. Hence the relative error attains larger values as in the linear discretized case, which can be seen in Fig.17.

Here we again plotted the relative error (linked with a solid red line) with the errorbars, obtained in the averaging prozess (normed by I_{exact}). We recognize, that the relative error and the errorintervals approximatly stay constant. When we compare this plot with Fig. 11, we see that the relative error is up to approximatly 200 times larger than the error obtained using the linear discretization. As the relative error stays constant and I_{exact} grows linear for small values of V , we attain the best match for small V -values, as the absolute error gets minimal, which can also be seen in Fig.16. One also recognizes that the perfect case ($I_{exact} - \langle I_s \rangle = 0$), still stays in the

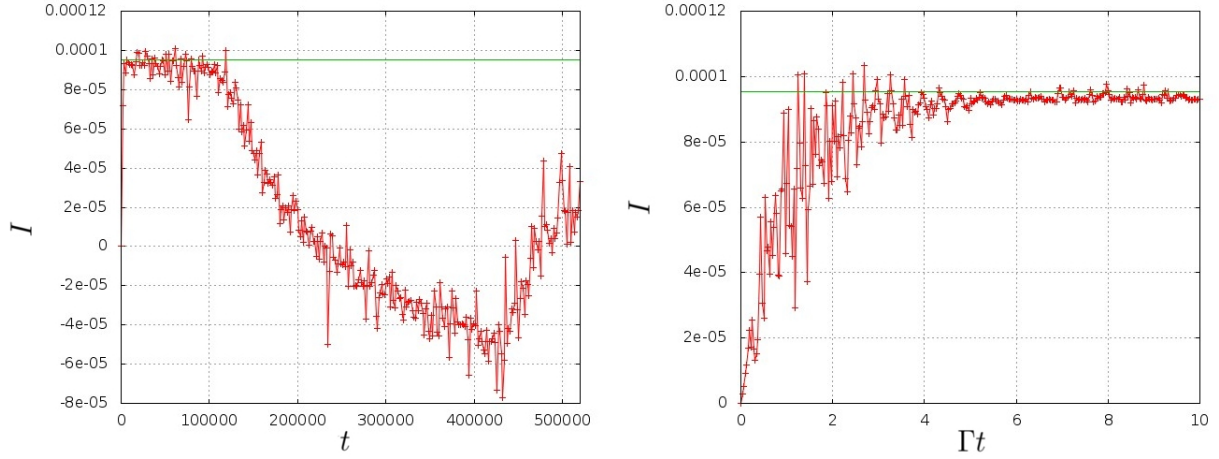


Figure 15: Long and short time regime for $\Gamma = 1e - 03$ (same as figure 13 otherwise)

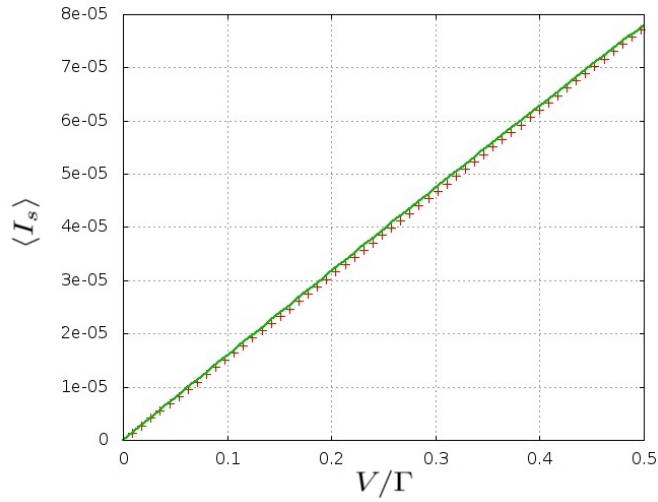


Figure 16: $\langle I_s \rangle(V)$ -plot for $\Gamma = 1e - 03$

errorintervals for all computed values of V . Because of that it is also justified to use the logarithmic discretization for the considered values of V . Especially in the conductance quantum regime we obtain excellent results for the logarithmic discretization (for $\Lambda = 1.1$), too.

13 $V/\Gamma > 1$ and $\Lambda = 2$

In the previous chapters, we tested our two discretizations for $V/\Gamma < 1$. In this regime, where the $I_{exact}(V)$ dependence is approximately linear, we attained excellent match with the theoretical result for both of our discretizations. Now one supposes, that with V/Γ growing, the logarithmic discretization will provide worse and worse results. To probe this we set $\Gamma = 5e - 03$ and use $M = 4011$, $a = 2$, $\Lambda = 2.5$ (this implies $\delta = 3.996e - 04$) for the linear discretization, and again $M = 803$ and $\Lambda = 1.1$ for the logarithmic one.

For $V/\Gamma = 8$ (see Fig. 18), we can still use both of our discretizations, as they attain a good

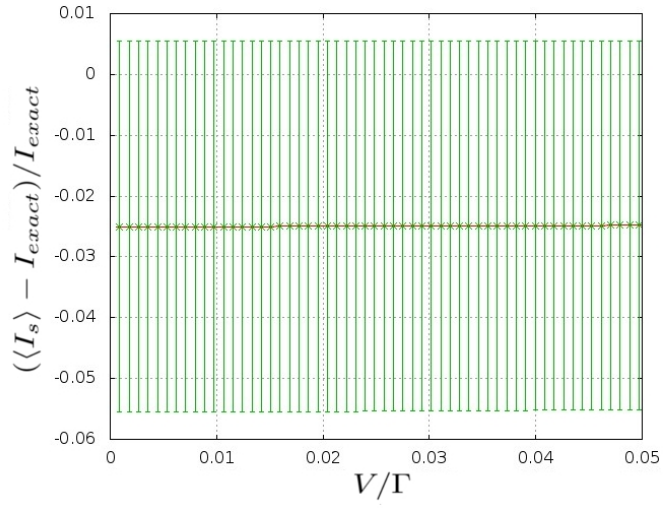


Figure 17: Relative error of logarithmic discretization for $\Gamma = 0.01$

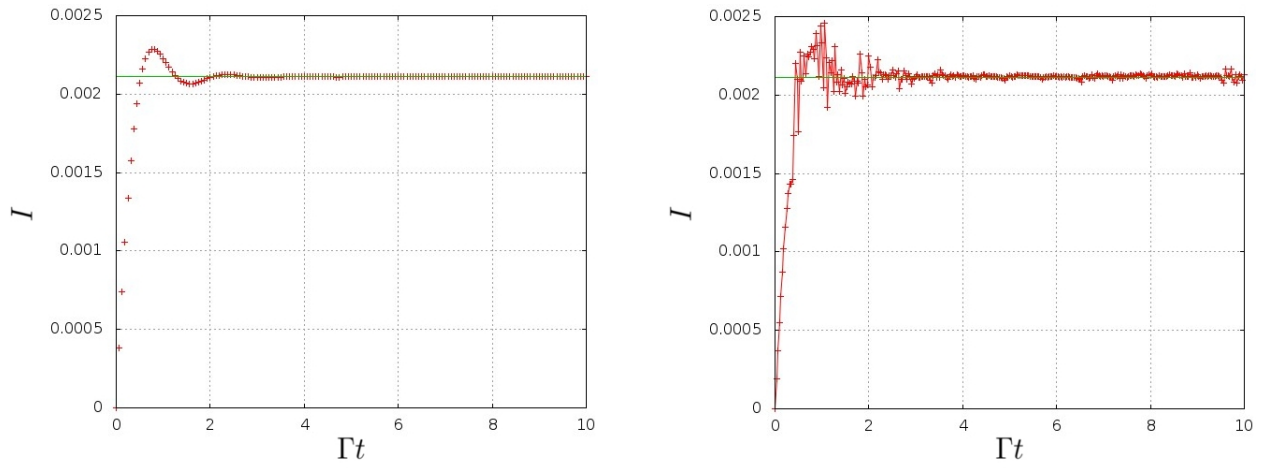


Figure 18: $V/\Gamma = 8$, linear (left) and logarithmic discretization (right) with theoretical result (solid green line)

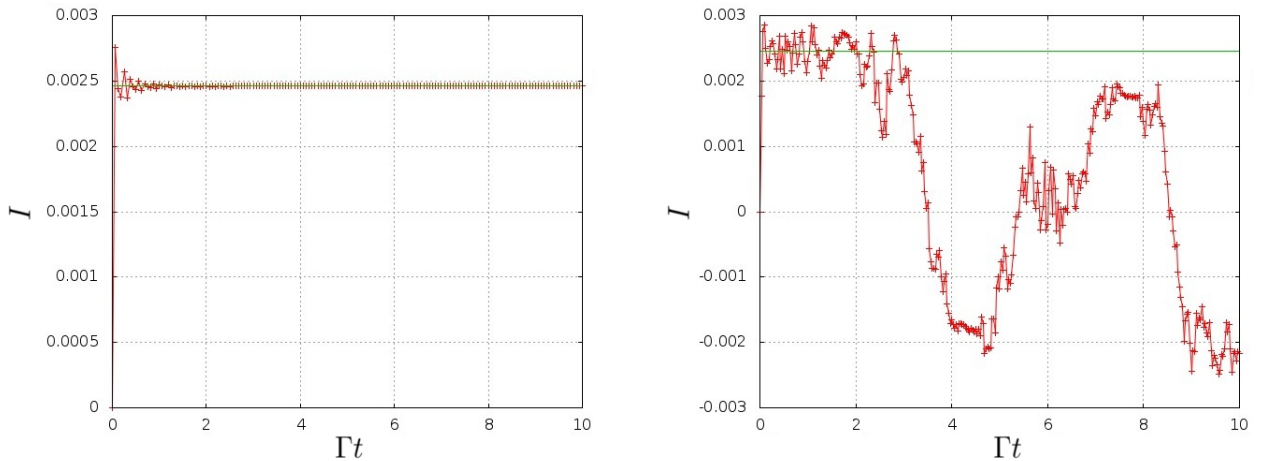


Figure 19: $V/\Gamma = 80$, linear (left) and logarithmic discretization (right) with theoretical result (solid green line)

steady state behavior. On top of that the both discretizations show an excellent match to the theoretical result (solid green line).

For larger values of V/Γ (see Fig. 19), we recognize two effects. The first one is, that the transient behavior is no longer dominated by $\frac{1}{\Gamma}$, but by $\frac{1}{V}$, as the applied electrical potential shortens the time, an electron stays in the d-level. The second effect is, that the two discretizations show big difference. While the linear discretization still behaves nice, the logarithmic one starts to bounce. Now we introduce another timescale $\tilde{\tau}(V)$, which is the time, one electron needs to pass from left to right when the potential V is applied. For that purpose we use the theoretical result (Eq.(128)) and attain:

$$\tilde{\tau}(V) = \frac{1}{\frac{\Gamma}{\pi} \arctan\left(\frac{V}{2\Gamma}\right)} \quad (151)$$

In figure 19 the applied potential $V = 0.4$ and therefore $\tilde{\tau} \simeq 2\Gamma$. Now we see that the current changes sign in a time of the order of $\tilde{\tau}$ in the logarithmic discretization case. This is an effect of discretization, as the current is forced to change sign, when one electron changed from left to right. It can be declared by the fact, that well resolved areas in one lead hit bad resolved (only one level) in the other (see Fig.12) for big values of V . But it is still justified to determine $\langle I_s \rangle$ for the logarithmic discretization as the current still shows steady state behavior. Hence we can use the logarithmic discretization even for $V/\Gamma \sim 100$, when $\Lambda = 1.1$.

For the numerical renormalization group Λ -values of approximately 2 are needed (see Ref.[1]). When we do the $I(t)$ -plot in this regime ($M = 803$), we attain figure 20, where we used $V/\Gamma \simeq 1$. When we compare this plot with the right plot of Fig.18, we recognize that we attain much more noise and we already get reflexions (negative current values) for times smaller than $\tilde{\tau}$ (here $\tilde{\tau} \simeq 6\Gamma$). However, one can already attain a $\langle I_s \rangle$ -value close to the theoretical result, when averaging $\Gamma t \in [2; 6]$. The same behavior can be observed for $V/\Gamma \ll 1$.

But for $V/\Gamma \geq 10$ (see Fig.21), the results are no longer satisfying as the $I(t)$ -plot no longer shows a nice steady state behavior and therefore it is hard to determine an interval for averaging. And

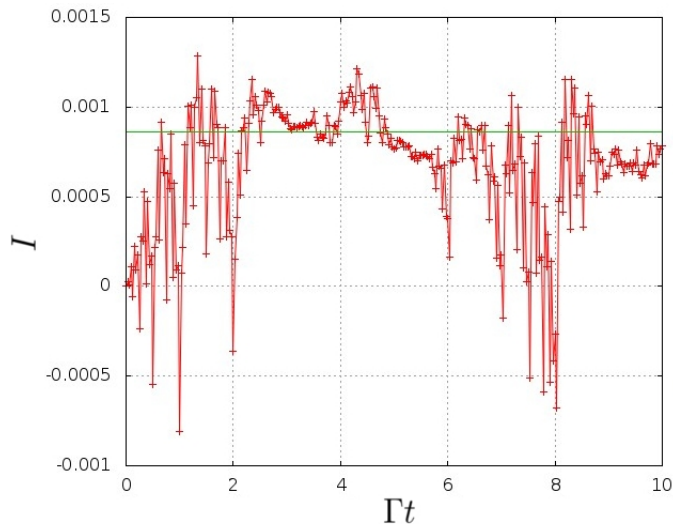


Figure 20: $I(t)$ -plot for $\Gamma = 5e - 03$, $V = 6e - 03$ and logarithmic discretization with $\Lambda = 2$.

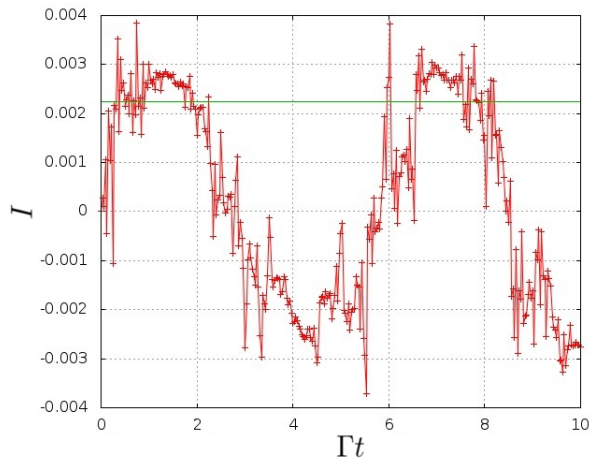


Figure 21: $I(t)$ -plot for $\Gamma = 5e - 03$ and $V = 0.06$ ($\Lambda = 2$).

even if one takes the interval around the first maximum of this plot, one would get a $\langle I_s \rangle$ -value larger than I_{exact} and this is not physical, as the theoretical result was developed in the continuum limit. Besides of that we can again observe the effects of discretization, as the current again changes time in the order of $\tilde{\tau}$ ($\simeq 2$).

Conclusion

To summarize, we can state, that the linear discretization had been the "better one" to simulate a continuous band, referring to the theoretical result. The $I(t)$ -plots showed really nice behavior for $V/\Gamma \simeq 1e - 08$ up to $V/\Gamma \simeq 100$ for different values of Γ .

On the other hand the $I(t)$ -plots of the logarithmic discretization showed much more noise and the

treatment had therefore been more complicated. However one can state that this discretization also shows good results for the $\Lambda = 1.1$ case, apart of the absolute error being larger than in the linear case. For $\Lambda = 2$, our plots are even more catchier to handle, as the noise increases further. In this case we attained reliable results for V/Γ -values up to 1. Entering the regime $V/\Gamma > 10$ we can no longer determine the steady state value, as the $I(t)$ -plot can no longer be approximated by a constant function in a timeinterval of necessary length ($\tilde{\tau}$).

Concluding we state that one can attain excellent results in the regime of small V for linear and logarithmic discretization ($\Lambda = 1.1$ or $\Lambda = 2$), while the discrepancy between the "better" linear and the "worse" logarithmic discretization grows for V getting bigger, dependent of the Λ -value of the logarithmic discretization.

Appendix

A Programs

A.1 Linear discretization

The program H1matrix.m produces the H -matrix for our linear discretization, using the same names of variables as in section 9 and in the last line the V_{all} vector of (126).

H1matrix.m:

```

1 M=803;lambda=1.1;
  a=80;
3 gamma=0.005;
  N=round((M-1)/2);
5 n=round((N-1)/2);
  % building epsilon_k's
7 for m=1:a
    ew(m)=-lambda**(-m+1);
9 endfor
  delta=abs(ew(a)/(n+1-a));
11 ew2=ew;
  for m=(a+1):n
13    ew2(m)=ew2(m-1)+delta;
  endfor
15 ew2=[ew2 0 -ew2(n:-1:1)];
  % building density of states rho_k
17 for m=2:(N-1)
    rho(m)=2/(ew2(m+1)-ew2(m-1));
19 endfor
  rho(N)=1/(ew2(N)-ew2(N-1));
21 rho(1)=rho(N);
  % building V_k's
23 for m=1:N
    V(m)=sqrt(gamma/(2*pi*rho(m)));
25 endfor
  Vdeg=V';
27 % constructing H-matrix and V_all vector
H=[diag(ew2) Vdeg zeros(N); V 0 V(N:-1:1) ; zeros(N) Vdeg(N:-1:1) diag(ew2(N:-1:1))];
29 V_all=[Vdeg ;-Vdeg];

```

The program `current1.m`, includes the function "current1", which determines the current according to equation (129). S, L and $Sdeg = S^\dagger$, are needed, as we construct $U(t)$ according to Eq.(144) as:

$$U(t) = e^{-iHt} = Se^{-iLt}S^\dagger \quad (152)$$

where $H = SLS^\dagger$ and L is diagonal.

`current1.m`:

```

1 function I0=current1(t,S,L,Sdeg,V_all,V)
3 M=length(S);
  N=round((M-1)/2);
5 n=round((N-1)/2);
  % built U and Udeg matrices
7 a=exp(-i*t*diag(L));
  A=diag(a);
9 U=S*A*Sdeg;
  Udeg=U';
11 % construct {k_start}={1,...,ll}u{lr,...,M}
  ll=round(n+1+(V/(2*delta)));
13 lr=round(M-n+(V/(2*delta)));
  % construct Ud vector
15 Ud=[U(N+1,1:ll) U(N+1,N+1) U(N+1,lr:M)];
  % construct U_tilde matrix
17 U_tilde=[Udeg(1:ll,1:N) Udeg(1:ll,(M-N+1):M) ; Udeg((N+1),1:N) Udeg((N+1),(M-N+1):M) ;
           Udeg(lr:M,1:N) Udeg(lr:M,(M-N+1):M)];
19
21 I0=-imag(Ud*U_tilde*V_all);
endfunction

```

The program `tI1plot.m` produces the $(t, I(t))$ -tupels for the $I(t)$ -plot for a certain electrical potential V .

`tI1plot.m`

```

[S,L]=eig(H);
2 Sdeg=S';
  % getting S,L,Sdeg
4 t=-125000;
  %set time starting value
6 for m=1:41
  t=t+125000;
8 x(m)=t;
  y(m)=current1(t,S,L,Sdeg,V_all,1e-05);
10
endfor
12 % gives back the x-vector containing timevalues
  % and y-vector containing corresponding current values for potential V=1e-05

```

The program `VI1plot.m` produces the $(V, I(V))$ -tupels for the $I(V)$ -plot by averaging the middle of the first steady state interval (see figure 8).

`VI1plot.m`:

```

1 [S,L]=eig(H);
M=length(S);
3 N=round((M-1)/2);
n=round((N-1)/2);
5 Sdeg=S';
V=0;
7 % starting value for the electrical potential
for l=1:60
9 V=V+2*delta;
x(l)=V;
11
% determine I(t)-values
13 t=0;
q=0;
15 z=zeros(81)(1,:);
for m=1:80
17 t=t+18750;
z(m+1)=current1(t,S,L,Sdeg,A,V-,V);
19 % finding boundaries of the first steady state interval
if z(m+1)*z(m)<0
21 q=m;
endif
23 endfor
% construction of the average interval
25 Q1=round((q+1)/2-20);
Q2=round((q+1)/2+20);
27 z=z(Q1:Q2);
y(1)=mean(z);
29 w(1)=std(z);
endifor
31 X=[x' y' w'];
% gives back the matrix X, containing the V-values,
33 % the I(V)-values and the variance of the averageing process

```

A.2 Logarithmic discretization

Due to our logarithmic discretization, our H -matrix will be dependent of the electrical potential V . Therefore the program H2func.m includes the function "H2func", which takes the V -value and gives back the $H = H(V)$ -matrix and the V_{all} -vector (see (126)).

H2func.m:

```

1 function [H, V_all]=H2func(V)
M=803;
3 N=round((M-1)/2);
n=round((N-1)/2);
5 % construction of epsilon_tilde_k
lambda=1.1;
7 gamma=0.005;
for k=1:n
9 ew(k)=-lambda**(-k+1);
endifor
11 ew2=[ew 0 -ew(n:-1:1)];
% translation of epsilon_tilde_k
13 ewl=ew2+(V/2);
ewr=ew2-(V/2);
15
% construction of rho_k
17 for m=2:(N-1)
rho(m)=2/(ew2(m+1)-ew2(m-1));
19 endfor
rho(N)=1/(ew2(N)-ew2(N-1));

```

```

21 rho(1)=rho(N);
% construction of V_k
23 for m=1:N
    V(m)=sqrt(gamma/(2*pi*rho(m)));
25 endfor
Vdeg=V';
27 % construction of H-matrix and V_all
H=[diag(ewl) Vdeg zeros(N); V 0 V(N:-1:1) ; zeros(N) Vdeg(N:-1:1) diag(ewr(N:-1:1))];
29 V_all=[Vdeg ; -Vdeg(N:-1:1)];
endfunction

```

The program current2.m is analogue to current1.m, with the difference, that the function "current2" doesn't depend on V , as the V -dependence is carried by the H -matrix in this discretization.

current2.m:

```

function I0=current2(t,S,L,Sdeg,V_all)
2
M=length(S);
4 N=round((M-1)/2);
n=round((N-1)/2);
6 % construction of U(t)
a=exp(-i*t*diag(L));
8 A=diag(a);
U=S*A*Sdeg;
10 Udeg=U';
% construction of Ud-vector
12 Ud=[U(N+1,1:(n+1)) U(N+1,N+1) U(N+1,(M-n):M)];
% construction of U-tilde matrix
14 Udegik=[Udeg(1:(n+1),1:N) Udeg(1:(n+1),(M-N+1):M) ; Udeg((N+1),1:N) Udeg((N+1),(M-N+1):M) ;
          Udeg((M-n):M,1:N) Udeg((M-n):M,(M-N+1):M)];
16 I0=-imag(Ud*Udegik*V_);
18 endfunction

```

The program tI2plot.m is analogue to tI1plot.m and therefore produces the $(t, I(t))$ -tupels for a certain electrical potential V , too.

tI2plot.m:

```

1 V=1e-05;
[H,V_all]=H2func(V);
3 [S,L]=eig(H);
Sdeg=S';
5 t=-3.125;
for m=1:321
7     t=t+3.125;
    x(m)=t;
9     y(m)=Stromneu(t,S,L,Sdeg,A,V_all);
11 endfor
% gives back the x-vector, including timevalues,
13 % and the corresponding y-vector, including current values.

```

The program VI2plot.m is analogue to VI1plot.m, with the difference, that we don't determine the average-interval for different values of Γ , but use $\Gamma t \in [5; 7]$ according to equation (150).

VI2plot.m:

```

1 V=0;
  % starting value for the electrical potential
3 for l=1:60
    V=V+2*delta;
5    x(1)=V;
    [H, V_all]=H2func(V);
7    M=length(H);
    [S,L]=eig(H);
9    Sdeg=S';
    % determining I(t) values of the averaging-interval
11   t=993.75;
    for m=1:81
13       t=t+6.25;
        z(m)=current2(t,S,L,Sdeg,V_all);
15   endfor
    y(1)=mean(z);
17   w(1)=std(z);
endfor
19 X=[x' y' w'];
  % gives back the matrix X, containing the V-values,
21 % the I(V)-values and the variance of the averageing process

```

References

- [1] The renormalization group: Critical phenomena and the Kondo problem, Wilson, Kenneth G., Rev. Mod. Phys., 47, 4, 773–840, 1975, Oct, 10.1103/RevModPhys.47.773, <http://link.aps.org/doi/10.1103/RevModPhys.47.773>, American Physical Society
- [2] Quantum Kinetics in Transport and Optics of Semiconductors, Haug, H. and Jauho, A.P., Bd. 6, 9783540735618, 2007931202, Springer Series in Solid-State Sciences, <http://books.google.de/books?id=w1am24ZE9jQC>, 2008, Springer
- [3] Grundkurs Theoretische Physik 7: Viel-Teilchen-Theorie, Nolting, W., 9783540241171, Springer-Lehrbuch, <http://books.google.de/books?id=pYDwdkBosDcC>, 2005, Springer

Acknowledgements

I want to thank Prof. Jan von Delft for giving me the possibility to work on this interesting topic and for inducting me to a field, which had been new for me.

In particular I want to thank Andreas Weixelbaum for all the interesting discussions and for always having time for me.

Erklärung

Hiermit versichere ich, dass ich die vorliegende Arbeit selbstständig und ohne fremde Hilfe angefertigt und nur die im Literaturverzeichnis aufgeführten Quellen verwendet habe.

München, den 06.August 2012